Physics of the Solid State, 2024, Vol. 66, No. 1

04,09

Photoactive paramagnetic centers in ZnO single crystals with an admixture of iron, vanadium or manganese

© V.A. Vazhenin[1], M.Yu. Artyomov[1], A.P. Potapov[1], L.E. Li[2], A.V. Fokin[1]

[1] Ural Federal University (Institute of Natural Sciences and Mathematics),
Yekaterinburg, Russia
[2] Shubnikov Institute of Crystallography „Crystallography and Photonics" Russian Academy of Sciences,
Moscow, Russia

E-mail: Vladimir.Vazhenin@urfu.ru

Received November 22, 2023
Revised November 22, 2023
Accepted November 24, 2023

In ZnO : Fe, ZnO : Mn, ZnO : V single crystals, the effect of irradiation with light with an energy of 1.32−3.0 eV on the EPR spectra of Fe^{3+} and Mn^{2+} centers was studied. In ZnO : Fe and ZnO : V the appearance of O^- hole centers localized near $^7Li^+$ ions in the positions of Zn^{2+} ions was observed, accompanied by the charge exchange $Fe^{3+} \rightarrow Fe^{2+}$. In ZnO : Mn, upon illumination, a change in the structure of the spectrum of forbidden Mn^{2+} transitions was detected.

Keywords: zinc oxide, impurity centers, paramagnetic resonance, influence of lighting.

DOI: 10.61011/PSS.2024.01.57855.259

1. Introduction

$II-VI$ semiconductors doped with $3d$-metal impurities have been extensively studied for many years to understand the crystal energy structure to facilitate modification of luminescent, magnetic, optical, photocatalytic and other properties of semiconductors. Hexagonal ZnO became one of the most promising materials among $II-VI$ semiconductors in optoelectronics and spintronics applications. Over two previous decades, absorption, photoconductivity and photoluminescence spectra have been studied in bulk samples as well as in thin films and nanocrystals. Zinc oxide is a direct band gap semiconductor with a 3.37 eV band gap at room temperature. ZnO has a wurtzite crystalline structure with space group $P63mc$. Each Zn^{2+} ion is surrounded by four O^{2-} ions located in the vertices of a tetrahedron deformed along the crystal axis c (point symmetry group $6mm$).

Electron paramagnetic resonance (EPR) provides the information about ground state energy spectrum, position symmetry and molecular structure of impurity $3d$-metals.

ZnO single crystals with iron impurity were investigated by the EPR method in [1–7]. The authors of [1–3] measured the spectra of samples grown from the gas phase, found trigonal Fe^{3+} centers (electron spin $S = 5/2$) and determined the spin Hamiltonian parameters of the isolated iron ions.

The authors of [4] examined the ZnO samples grown by chemical vapor transport and doped with iron and lithium by means of diffusion. Besides the trigonal Fe^{3+} centers, the EPR spectrum of these crystals after lithium-doping had three additional centers of trivalent iron ions. The detected centers were surely assigned to dimer $Fe^{3+}-Li^+$ centers that differ from each other in relative positions of iron and lithium ions occupying cation positions.

Detailed examination conducted in [5,6] on the EPR spectra of ZnO : Fe^{3+} single crystals grown by the hydrothermal method has detected trigonal and low-symmetrical dimer Fe^{3+} centers observed by the authors of [4] before. ZnO crystals grown by the hydrothermal method always contain a lithium impurity due to the process features [8]. Spin Hamiltonian of all four types of centers were determined by means of orientation behavior measurements of resonance transition positions. The authors believed that low-symmetrical centers occur as a result of association of Fe^{3+} ions with Zn^{2+} or O^{2-} vacancies which apparently contradicts the conclusions of [4].

The authors of [7] used the electron-nuclear double resonance spectroscopy to determine the chemical nature of the impurity bound with Fe^{3+} in the hydrothermal zinc oxide. The measurements showed that NMR transitions on all dimer Fe^{3+} centers corresponded to nuclei with g-factor $g_N = 2.171$ and spin $I = 3/2$ which is explicitly indicative of the presence of a lithium ion in close vicinity of Fe^{3+}.

The effect of X-ray and UV irradiation of lithium-doped zinc oxide crystals containing an uncontrolled iron impurity was studied in [8,9]. After irradiation of samples at liquid nitrogen temperature, the EPR spectrum occurred due to four hole centers O^- surrounding lithium ions in Zn^{2+} positions, while Fe^{3+} centers losing their intensity.

EPR spectra of V^{2+} ($S = 3/2$, $I = 7/2$, natural abundance 100%) and V^{3+} ($S = 1$) centers in ZnO were studied by the authors of [10–12], V^{2+} signals could be detected at temperatures below 22 K and V^{3+} centers were observed below 120 K [12]. Fine and hyperfine structure parameters were determined for these centers.

Zinc oxide with manganese impurity was stuied in [13–16]. Mn^{2+} (S = 5/2, nuclear spin I = 5/2, abundance 100%) have a resolved hyperfine structure and zero field splitting smaller than Fe^{3+}.

This work is devoted to the EPR study of photosensitive centers in single crystals of zinc oxide doped with iron, vanadium or manganese.

2. Experimental procedure

ZnO : M (M — Mn, Fe or V) single crystals were produced by the hydrothermal method in $ZnO{-}M_xO_y{-}KOH{-}LiOH{-}H_2O$ systems. Impurity concentration in the initial system was equal to 2%. Lithium hydroxide was added to the system to improve oxide stoichiometry and crystal quality due to partial substitution of Zn^{2+} by Li^+ Reducing environment in the hydrothermal synthesis ensured transition Mn^{3+} (Fe^{3+}) → Mn^{2+} (Fe^{2+}) [17–19].

The EPR spectra at room temperature and 100−120 K were measured using EMX Plus Bruker X-band spectrometer in fields up to 1450 mT. The samples were placed into a PTFE barrel rotating in a vertical plane and mounted on a standard goniometer rod to provide high-accuracy orientation of the magnetic field. Low-temperature measurements were carried out using a standard nitrogen temperature control system.

The samples were illuminated by visible (FYL-5013VC1C violet LEDs with peak wavelength 413 nm, green L-7113VGC — 525 nm, yellow L-7113SYC — 588 nm, red L-7113SRC-F — 640 nm) and infrared (L-7113F3C — 940 nm) light sources. The samples were illuminated through a standard window of the spectrometer microwave cavity.

3. Results and discussion

ZnO : Fe samples at 300 K demonstrated intense and highly broadened EPR signals of four Fe^{3+} centers and quite intense sextets of the hyperfine structure of Mn^{2+} centers. In ZnO : V crystals, spectra of Fe^{3+} and Mn^{2+} centers were observed that were more suitable for signal analysis near $g = 2$ than those in ZnO : Fe. The spectrum of ZnO : V at room temperature is shown in Figure 1, where transitions of all Fe^{3+} centers are marked whose positions are well described by the fine structure parameters [5]. Moreover, unknown signals with g-factors 2.004 and 2.06 were detected in orientation $\mathbf{B} \parallel \mathbf{c}$ and were observed both at room temperature and at 100 K. There was no signal with $g = 2.004$ in ZnO : Fe crystal.

In ZnO : Fe and ZnO : V samples at 100 K and $\mathbf{B} \parallel \mathbf{c}$, satellites spaced away at 0.5 mT were detected at the central transition of the isolated Fe^{3+} center (width 0.15 mT). Ratio of peak intensities of the central signal and satellites was approximately equal to 100. Considering the findings in [1], these satellites should be assigned to the hyperfine structure of ^{57}Fe isotope (S = 1/2, natural abundance 2.2%).

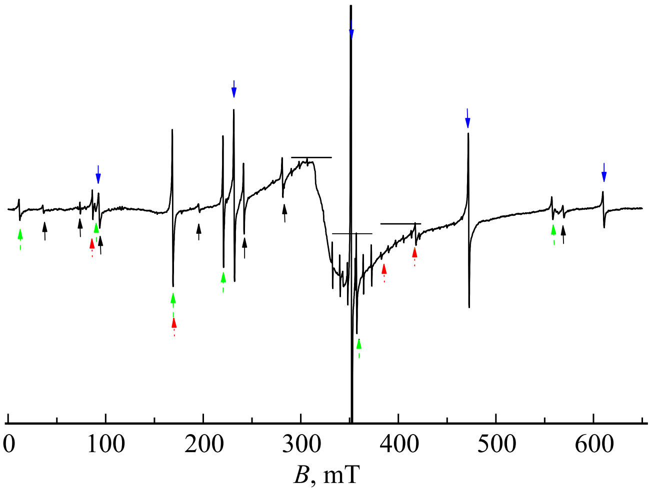

Figure 1. EPR spectrum of ZnO : V crystal in orientation $\mathbf{B} \parallel \mathbf{c}$ (B — magnetic field induction) at room temperature at 9875 MHz. Upper blue arrows — calculated positions of transitions of the isolated Fe^{3+} ion, black solid arrows — calculated positions of Fe−Li1 centers, green dashed arrows — Fe−Li2, red dashed arrows — Fe−Li3 with parameters [5] in the notations [7]. Horizontal segments show field ranges where hyperfine components of transitions $-1/2 \leftrightarrow +1/2$ and $\pm 1/2 \leftrightarrow \pm 3/2$ of centers Mn^{2+} are observed. Long broad signal in the center is due to the sample holder and cavity.

Vanadium ion signals in ZnO : V were not detected. The V^{3+} centers in the crystal likely have very low concentration, while V^{2+} signals are not observed due to high measurement temperature [12].

In ZnO : Mn, trigonal Mn^{2+} center spectrum dominated, but weak signals of Fe^{3+} centers were also observed. Similar type of the spectrum was reported in [20–21]. Fine and hyperfine structures of Mn^{2+} center spectrum were described by trigonal spin Hamiltonian [22]:

$$H = g\beta(\mathbf{BS}) + 1/3(b_{20}O_{20}) + 1/60(b_{40}O_{40} + b_{43}O_{43}) + (\mathbf{S}A\mathbf{I}), \qquad (1)$$

where g is g-factor, β is Bohr magneton, $\mathbf{S}$ is the electron spin operator, I is the nuclear spin operator, $b_{\rm nm}$ are fine structure parameters, $O_{\rm nm}$ are Stevens spin operators, A is the hyperfine interaction parameter. Minimization of rms deviation F of calculated frequencies from experimental ones at 120 K, including both allowed and forbidden transitions in orientations $\mathbf{B} \parallel \mathbf{c}$ and $\mathbf{B} \perp \mathbf{c}$ resulted in the following values (1):

$$g = 2.0012, \quad b_{20} = -695.8, \quad b_{40} = -5.6,$$

$$b_{43} = \pm 175.2, \quad A = -222.1 \quad (b_{\rm nm} \text{ and } A \text{ in MHz}) \qquad (2)$$

with $F \approx 4$ MHz that slightly differ from those obtained in [20–21] at 300 K. Parameters of the isolated Fe^{3+} center

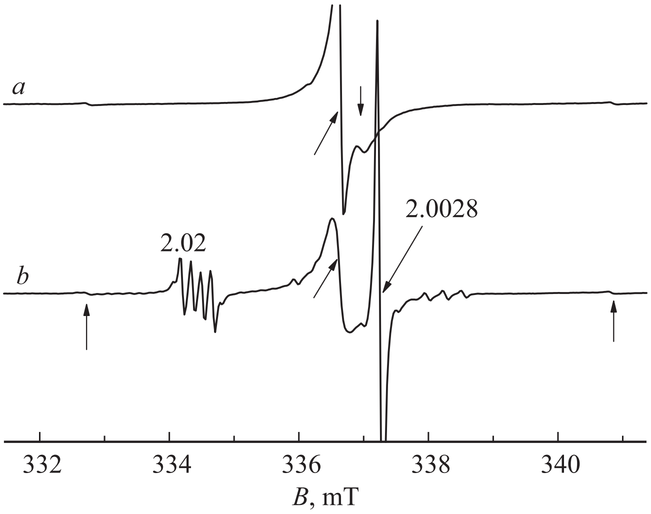

Figure 2. Central part of the EPR spectrum of ZnO : V crystal in orientation **B** || **c** at 100 K at 9453 MHz. *a* — in darkness, *b* — after illumination by violet LED. Lower inclined arrows indicate the signal of isolated Fe^{3+} centers, lower vertical arrows indicate the hyperfine structure components of transition $-1/2 - +1/2$ of Mn^{2+}, upper vertical arrow indicates the signal with $g = 2.004$.

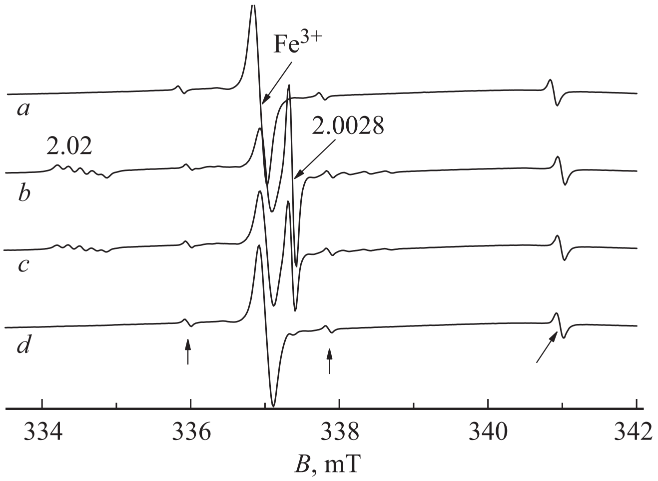

Figure 3. Central part of the EPR spectrum of ZnO : Fe crystal in the orientation close to **B** || **c** at 120 K at 9453 MHz. *a* — in darkness, *b* — after illumination by violet LED, *c* — green, *d* — yellow. Lower inclined arrow marks allowed transition Mn^{2+}, vertical arrow marks forbidden transitions Mn^{2+}. Signals with g-factors 2.02 and 2.0028 belong to $O^{-}-{}^{7}Li$ hole centers.

at 120 K are slightly lower than the values at 300 K [5]: $b_{20} = -1740.8$ MHz, $b_{40} = -36$ MHz.

Illumination of ZnO : V (or ZnO : Fe) samples with a violet LED at 100 K (at 120 K) during 5 min results in the occurrence of the signal quartet with a center at $g = 2.02$ and an intense singlet with $g = 2.0028$ in the EPR spectrum (see Figure 2). In Figures 2 and 3, transitions of the Mn^{2+} ion with $\Delta M = \pm 1$, $\Delta m = 0$, are referred to as allowed transitions, while transitions with $\Delta M = \pm 1$, $\Delta m = \pm 1$, are referred to as forbidden transitions, where M and m are electron and nuclear spin projections, respectively. In this case, the signal of transition $-1/2 - +1/2$ of the isolated Fe^{3+} with $g = 2.006$ apparently loses intensity as reported in [8–9,17–18]. In addition, weak non-identified signals with $g = 1.964$ and $g = 1.997$ occur.

Signals with g-factors 2.02 and 2.0028 (Figure 2), that occur with illumination, according to [8–9], belong to four types of O^{-} $(S = 1/2)$ hole centers adjacent to ${}^{7}Li^{+}$ isotopes $(I = 3/2$, abundance 92.6%) that replaced Zn^{2+} ions. The signal with $g = 2.0028$ is attributed to the O^{-} center, whose bond axis $O^{-}-Li^{+}$ is parallel to the magnetic field and the hyperfine interaction with the nuclear spin of ${}^{7}Li^{+}$ is very small [9]. Other three O^{-} centers in this field orientation are equivalent, their quartet spectrum structure is due to the interaction with the ${}^{7}Li^{+}$ nucleus. According to [9], when the sample is illuminated, the electron from O^{2-} adjacent to ${}^{7}Li^{+}$ moves to the conduction band and is trapped by Fe^{3+} (d^5) that transforms into Fe^{2+} (d^6), these are the processes that are responsible for the observed effects. Some weak signals around the transition of the parallel center O^{-} $(g = 2.0028)$ in Figure 2 are attributed to the interaction of its electron spin with the nuclear spin of the nearest ${}^{67}Zn^{2+}$ $(I = 5/2$, abundance 4.1%) [9].

Results of samples illumination with different LEDs are shown in Figure 3. As can be seen, with an increase in light wavelength, the effect (occurrence of O^{-} hole centers near ${}^{7}Li^{+}$ and decrease in the number of Fe^{3+} centers) decreases significantly, yellow illumination has almost no effect on the spectrum. Therefore, the energy required to form O^{-} hole centers is approximately equal to 2.3 eV.

When the illumination has been turned off, intensities of Fe^{3+} and O^{-} signals are recovered within several hours. Sample illumination with the energy of light 1.3–1.9 eV significantly accelerates the process (see Figure 4). Therefore, it is safe to say that the ground state of Fe^{2+} in

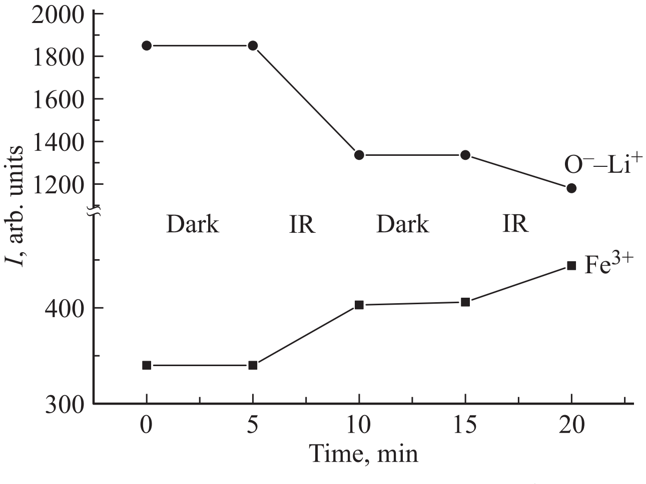

Figure 4. Dependence of peak intensities of Fe^{3+} and O^{-} signals at 105 K on time beginning from the violet LED turning off (see Figure 2) in dark and IR illumination conditions (940 nm).

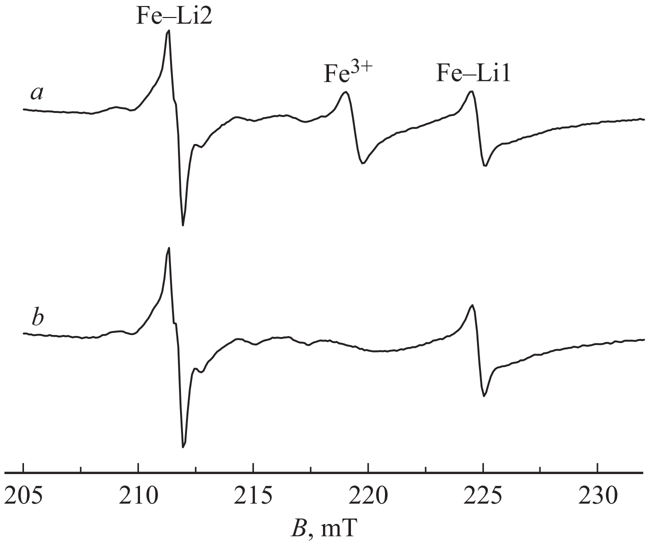

Figure 5. Transition $-1/2 \leftrightarrow -3/2$ of an isolatedisolated Fe^{3+} center and Fe$-$Li centers in a ZnO : V crystal in an orientation close to $\mathbf{B} \parallel \mathbf{c}$ at 100 K, at 9454 MHz. *a* — in darkness, *b* — after illumination with a violet LED.

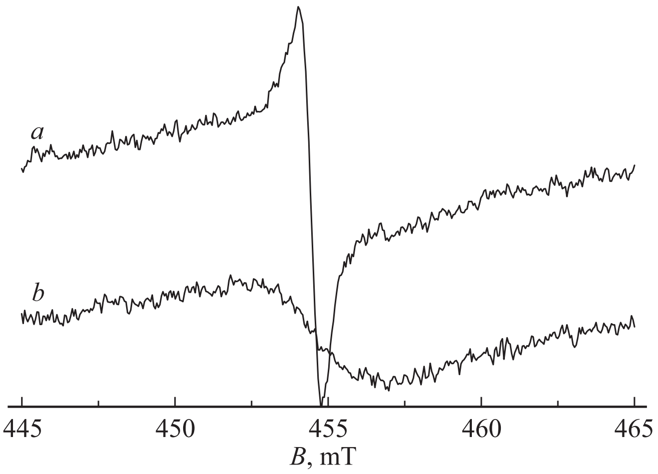

Figure 6. Transition $1/2 \leftrightarrow 3/2$ of a isolated Fe^{3+} center in ZnO : V crystal in orientation $\mathbf{B} \parallel \mathbf{c}$ at 100 K, at 9454 MHz. *a* — in darkness, *b* — after illumination with a violet LED.

ZnO is no more than 1.3 eV away from the bottom of the conduction band.

It is reasonable that a decrease in $-1/2 \leftrightarrow 1/2$ signal intensity of the isolated Fe^{3+} ion with illumination of samples is followed by a decrease in the intensity of other transitions of this center as well (see Figure 5). At the same time, it is important to note the constancy of the signal intensities of the locally compensated Fe$-$Li ions (Figure 5). The influence of illumination on the $1/2 \leftrightarrow 3/2$ transition of the isolated Fe^{3+} center as shown in Figure 6 suggests that the initial signal consists of two components. Narrow component with $\Delta B_{\text{pp}} = 0.8$ mT disappears during illumination, and wide component with $\Delta B_{\text{pp}} = 4.2$ mT scarcely responds to the illumination (ΔB_{pp} is the signal width between extrema of the first derivative). Integral signal intensity (Figure 6) decreases by 25% as a result of illumination due to the narrow component.

Existence of two types (components) of transitions of isolated Fe^{3+} centers may be explained by the fact that ZnO crystal, besides the impurity iron ions that do not have defects in the wide neighborhood, also contains „quasi-isolated“ Fe^{3+} centers associated with remote charge-compensating defects whose influence does not result in formation of single Fe$-$Li type centers (Figures 1, 4), but only broadens the EPR signals. It should be expected that the probability of trapping of an electron by quasi-isolated centers will be lower than by „truly“ isolated centers, because the potential well created by the dipole will be less extended that generated by a point charge. Apparently, Fe$-$Li centers will not trap an electron, because the dipole moment of such center is low and the electric charge is compensated.

Illumination of ZnO : Mn samples by green LED at 120 K in the $\mathbf{B} \perp \mathbf{c}$ orientation does not lead to significant variation of the EPR spectrum of the allowed transitions of Mn^{2+} as reported in [17–18]. At the same time, the signals of the isolated Fe^{3+} centers lose intensity as we have previously observed in ZnO : V samples. The signals of O^- hole centers cannot be detected due to their overlap with the intense allowed transitions of Mn^{2+}.

At $\mathbf{B} \perp \mathbf{c}$ in the 70$-$225 mT field range a rich EPR spectrum of forbidden hyperfine transitions of Mn^{2+} is observed. In its low-field part (70$-$150 mT), signals from different electronic transitions are highly overlapped. Therefore, Figure 7 shows the spectrum of only the high-field part of the forbidden transitions, both in darkness and under illumination. It can be seen that positions and intensities of a set of observed signals (Figure 7, *a*) are in good agreement with the calculation predictions (diagonalization of the 36th order complex matrix) with parameters (2) (see Figure 7, *d*). However, the spectrum contains additional groups of weak signals which grow significantly with illumination (marked with arrows of different colors in Figure 7, *c*), and the identified initial transitions lose their intensity. It should be noted that illumination of a sample by a yellow LED (also red LED) is more effective for the described process than illumination by a green LED (see Figure 7).

The attempt to describe the specified additional signals by a trigonal spin Hamiltonian (1) was unsuccessful, rms deviation increased by an order of magnitude compared with the result for the trigonal center. This fact suggests that additional transitions are attributed to centers with a lower symmetry. The observed signal asymmetry in this spectrum speak in favor of the existence of several additional centers. As with the existence of two kinds of isolated Fe^{3+} centers, some Mn^{2+} ions likely have defects in their vicinity that reduce the symmetry of center and change the EPR spectrum. Therefore, there are truly isolated as well as several quasi-isolated Mn^{2+} centers that differ both in the type of defect and its position relative to manganese. Sample

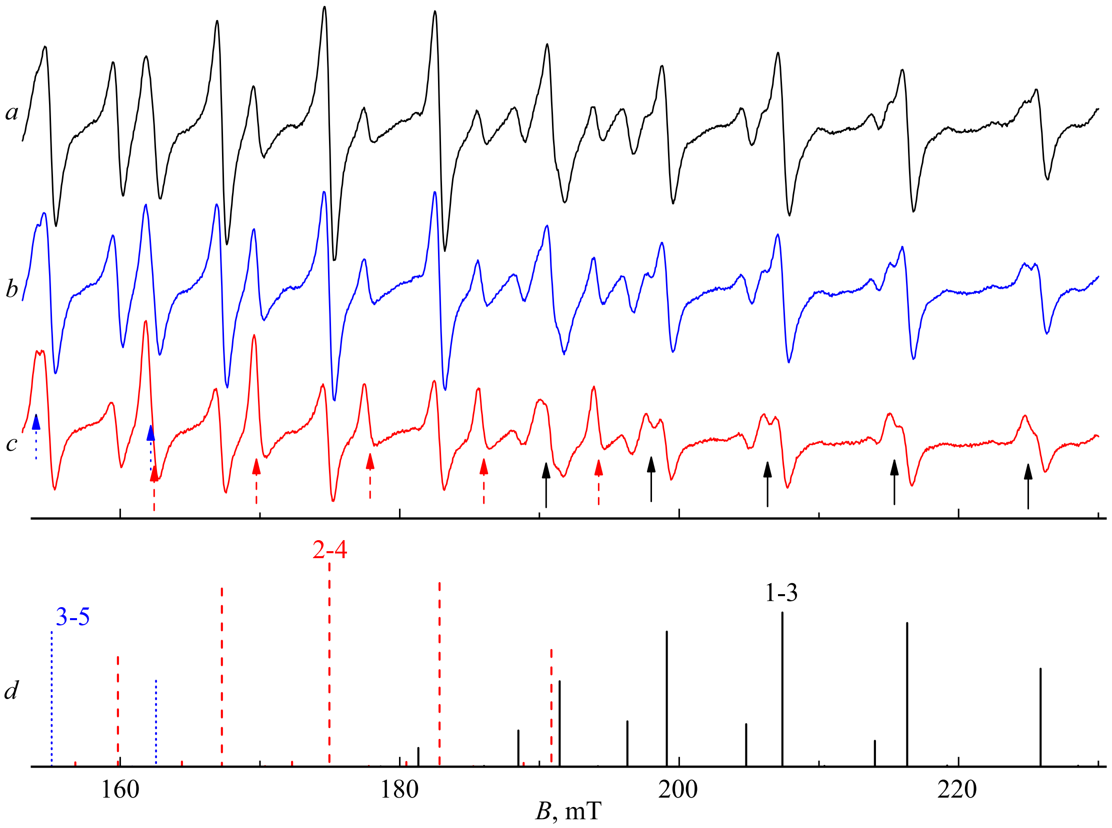

Figure 7. Hyperfine forbidden transitions of Mn^{2+} centers at 120 K in orientation $\mathbf{B} \perp \mathbf{c}$ orientation. *a* — in darkness, *b* — under illumination with a green LED, *c* — with yellow LED illumination, *d* — calculated positions and intensities of transitions with $\Delta M = \pm 2$ (transitions between levels 1-3 — black solid lines, 2-4 — red dashed lines, 3-5 — blue dotted lines, numeration of electronic levels is from bottom to top here).

exposure to light results in the occurrence of an additional number of defects (not necessarily observed in EPR), therefore, concentration of quasi-isolated centers grows and the number of truly isolated centers decreases. O^- hole centers are probably not able to be such defects, because yellow LED illumination almost does not influence their concentration. Additional investigations are required to define the origin and structure of quasi-isolated Mn^{2+} centers.

4. Conclusion

Exposure of ZnO : Fe, ZnO : V samples to 413–525 nm LED emission results in the occurrence of new line in the EPR spectra. These lines are attributed to O^- hole centers localized near $^7Li^+$ that substituted Zn^{2+}, the EPR spectrum intensity of Fe^{3+} decreases significantly. In case of exposure to 588 nm light, the specified effect is almost not observed. A conclusion has been made that the energy of generation of O^- hole centers associated with lithium ion is approximately equal to 2.3 eV. Exposure of the samples to light with energies within 1.32–1.94 eV significantly accelerates recovery of the spectrum.

In the EPR spectrum of forbidden Mn^{2+} ($\Delta M = \pm 2$) transitions in orientation $\mathbf{B} \perp \mathbf{c}$ when ZnO : Mn sample is exposed to green or yellow LED illumination, an increase in the signal intensity of the additional spectrum, likely attributed to low-symmetry Mn^{2+} centers having a defect in the vicinity, and a decrease in the intensity of the main spectrum of isolated Mn^{2+} ions were detected.

Funding

The study was financially supported by the Ministry of Science and Higher Education of the Russian Federation, topic No. FEUZ-2023-0017 using the equipment provided by Ural Common Use Center „Modern Nanotechnologies“ Ural Federal University (Reg. No. 2968).

Conflict of interest

The authors declare that they have no conflict of interest.

References

[1] W.M. Walsh, Jr., L.W. Rupp Jr. Phys. Rev. **126**, 952 (1962).
[2] J. Schneider. Z. Naturforsch. **17a**, 189 (1962).
[3] A. Hausmann. Solid State Commun. **6**, 457 (1968).
[4] W.C. Holton, M. de Wit, T.L. Estle, B. Dischler, J. Schneider. Phys. Rev. **169**, 359 (1968).

[5] D.V. Azamat, M. Fanciulli. Physica B **401–402**, 382 (2007).
[6] D.V. Azamat, J. Debus, D.R. Yakovlev, V.Y. Ivanov, M. Godlewski, M. Fanciulli, M. Bayer. Phys. Status Solidi B **247**, 1517 (2010).
[7] Yu.S. Kutin, G.V. Mamin, S.B. Orlinskii. J. Magn. Res. **237**, 110 (2013).
[8] J. Schneider, O. Schirmer. Z. Naturforsch. **18a**, 20 (1963).
[9] 0.F. Schirmer. J. Phys. Chem. Solids **29**, 1407 (1968).
[10] A. Hausmann, E. Blaschke. Z. Physik **230**, 255 (1970).
[11] G. Filipovich, A.L. Taylor, R.E. Coffman. Phys. Rev. B **1**, 1986 (1970).
[12] P. Schreiber, A. Hausmann. Z. Physik. **251**, 71 (1972).
[13] P.B. Dorain. **112**, 1058 (1958).
[14] J. Schneider, S.R. Sircar. Z. Naturforsch. **17a**, 570 (1962).
[15] J. Schneider, S.R. Sircar. Z. Naturforsch. **17a**, 651 (1962).
[16] A. Hausmann, H. Huppertz. J. Phys. Chem. Solids **29**, 1369 (1968).
[17] I.P. Kuzmina, V.A. Nikitenko. Okis tsinka. Poluchenie i opticheckie svoistva /Pod red. I.K. Vereshchagina. Nauka, M., (1984), 166 s. (in Russian).
[18] L.N. Demianets, D.V. Kostomarov, I.P. Kuz'mina, C.V. Pushko. Crystallogr. Rep. **47**, Suppl. *1*, S86 (2002).
[19] L.N. Dem'yanets, V.I. Lyutin. J. Cryst. Growth. **310**, 993 (2008).
[20] V.I. Sokolov, N.B. Gruzdev, V.A. Vazhenin, A.V. Fokin, A.V. Druzhinin. FTT **61**, 817 (2019). (in Russian).
[21] V.I. Sokolov, N.B. Gruzdev, V.A. Vazhenin, A.V. Fokin, A.V. Korolev, V.V. Men'shenin. ZhETF **157**, 1 (2020). (in Russian).
[22] S.A. Altshuler, B.M. Kozyrev. Elektronnyi paramagnitnyi rezonans soedineniy elementov promezhutochnykh grupp. Nauka, M., (1972), S. 121 (in Russian).

Translated by E.Ilinskaya